JoT JOURNAL OF TURBULENCE

http://jot.iop.org/

# Three-dimensional vorticity dynamics of miscible porous media flows†

**Amir Riaz and Eckart Meiburg‡**

Department of Mechanical and Environmental Engineering, University of California, Santa Barbara, CA 93106, USA
E-mail: ariaz@engineering.ucsb.edu and meiburg@engineering.ucsb.edu

Received 4 November 2002
Published 17 December 2002

**Abstract.** High accuracy three-dimensional numerical simulations are performed in quarter five-spot geometry to analyse miscible displacements with gravity override. Using a vorticity formulation, the coupling between viscous and gravitational effects is studied. Its is found that an optimal level of interaction among the viscous and gravity-related vorticity components leads to an improvement in displacement efficiency.

PACS numbers: 47.32.Cc, 47.55.Mh, 47.54.+r

JoT 3 (2002) 061

## Contents



† This article was chosen from Selected Proceedings of the 4th International Workshop on Vortex Flows and Related Numerical Methods (UC Santa-Barbara, 17–20 March 2002) ed E Meiburg, G H Cottet, A Ghoniem and P Koumoutsakos.

‡ Author to whom any correspondence should be addressed.

 PII: S1468-5248(02)54718-4 1468-5248/02/000001+7$30.00

## 1. Introduction

The stability of the interface between fluids of different viscosities in a porous medium has been a subject of investigation for a number of years, for both miscible and immiscible phase displacements [1]. The phenomenon of viscous fingering occurs when a more viscous fluid is displaced by a less viscous one. The interface between the two fluids becomes unstable and the less viscous fluid channels through and bypasses the more viscous fluid. If the two fluids differ also in density, then viscous and gravitational forces couple to influence the displacement process.

Pioneering work on fingering instability related to adverse mobility displacement was done by Hill [2], Saffman and Taylor [3] and Chouke *et al* [4]. A thorough understanding of the mechanisms of instability operative in the dynamical evolution of the interface is of prime importance for practical applications like in enhanced oil recovery, ground water hydrology and packed bed reactions.

Our objective is to study the relative effects of viscous and gravitational forces on the efficiency of the displacement process in terms of the interaction of related components of vorticity [5]–[9]. In a 3D setting, additional complexity is introduced due to varying levels of interaction between different spatial components of viscous and gravity-related vorticity.

## 2. Governing equations

We solve the 3D, miscible, homogeneous porous media problem in a quarter five-spot geometry. This configuration consists of a staggered array of injection and production wells modelled by line sources and sinks; figure 1(a). Since the flow is assumed to be symmetric across cell boundaries, a single cell represents the computational domain shown in figure 1(b). Darcy's law gives the velocity due to a pressure gradient across a porous medium, which in dimensionless form is

$$\boldsymbol{\nabla} p = -\mu \boldsymbol{u} + Gc\,\boldsymbol{\nabla} z \tag{1}$$

where $\mu$ is the local viscosity and $c$ is the concentration. Upon taking the curl of Darcy's equation a vorticity equation is obtained, equation (3), which contains two sources of vorticity production related to viscosity and gravity; therefore vorticity is present only where viscosity and density vary. An incompressible flow is assumed and the transport of concentration is given by a convection–diffusion equation. The set of governing equations is

$$\frac{\partial c}{\partial t} + \boldsymbol{u}\cdot\boldsymbol{\nabla} c = \frac{1}{Pe}\nabla^2 c \tag{2}$$

$$\boldsymbol{\omega} = R\,\boldsymbol{\nabla} c \times \boldsymbol{u} + \frac{G}{\mu}\,\boldsymbol{\nabla} z \times \boldsymbol{\nabla} c \tag{3}$$

$$\boldsymbol{u} = \boldsymbol{u}_p(x,y) + \boldsymbol{u}_r(x,y,z,t) \tag{4}$$

$$\boldsymbol{u}_r = \boldsymbol{\nabla} \times \boldsymbol{\psi} \tag{5}$$

$$\boldsymbol{\nabla}^2 \boldsymbol{\psi} = -\boldsymbol{\omega}. \tag{6}$$

Three dimensionless parameters appear in the above equations: the Peclet number $Pe = Q/D$, the viscosity parameter $R = -(1/\mu)\mathrm{d}\mu/\mathrm{d}c = \ln(\mu_2/\mu_1)$ and the gravity parameter $G = g(\rho_1 - \rho_2)kL/Q\mu_1$. Subscripts 1 and 2 refer to injected and displaced fluid respectively. $k$ is the constant permeability, $Q$ is the injection rate per unit depth and $D$ is the diffusion coefficient. The initial condition for the concentration is prescribed with a radial error function profile at time $t > 0$. The initial velocity is the potential component $u_p$ which arises due to the source and sink arrangement and gives rise to diverging (converging) streamlines close to the source (sink). A high accuracy numerical method is employed by using sixth-order compact finite differences

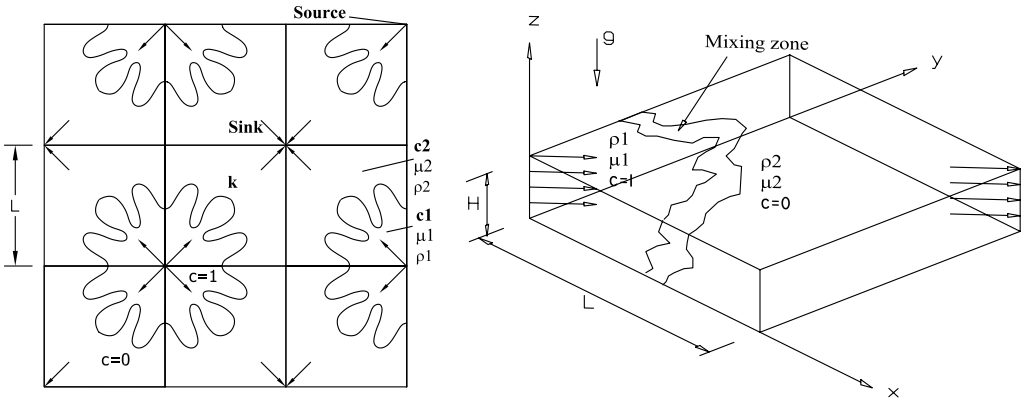


(a) (b)

**Figure 1.** (a) The layout of the quarter five-spot arrangement. (b) The computational domain.

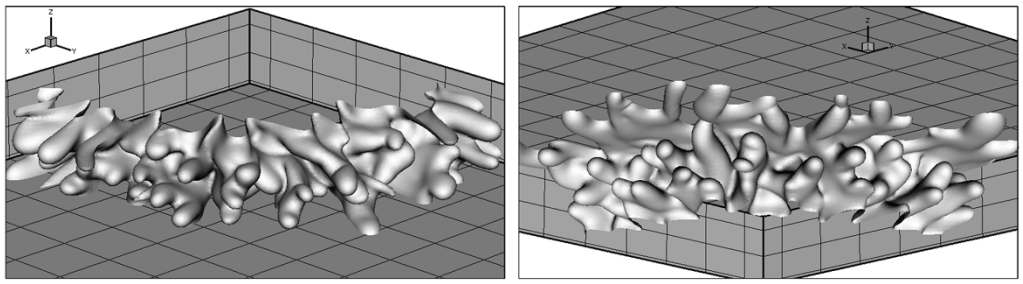

(a) (b)

**Figure 2.** Concentration isosurfaces for $Pe = 800$, $R = 2.5$ and $t = 0.14$. (a) $G = 0$, (b) $G = 0.5$.

for spatial derivatives [10]. Equation (6) is solved by Fourier–Galerkin discretization; typically, $512 \times 512 \times 64$ grid points are used. Equation (2) is solved with explicit third-order Runga–Kutta time integration and a CFL criterion determines the allowable time step which is of the order of $10^{-6}$. Vertical boundaries are symmetric and horizontal boundaries have zero normal flux. We define a breakthrough time when the concentration at the sink is 10% of the injected fluid.

## 3. Discussion of results

First consider an unstable displacement without density difference; figure 2(a). The initial wavelength and growth rate of perturbations are in agreement with linear stability analysis for radially symmetric flows [11]. The disturbances develop into viscous fingers that grow in time. When the amplitude of the fingers becomes large, they start to interact with each other. Several mechanisms of nonlinear finger interaction can be observed in figure 2(a), i.e. merging, shielding and coalescence [5], which accelerate the convective mixing of the interfacial regions. This brings about a relaxation of the concentration gradient and the overall vorticity level drops. Furthermore, such interactions lead to a reduction in the number and an increase in the size of the fingers.

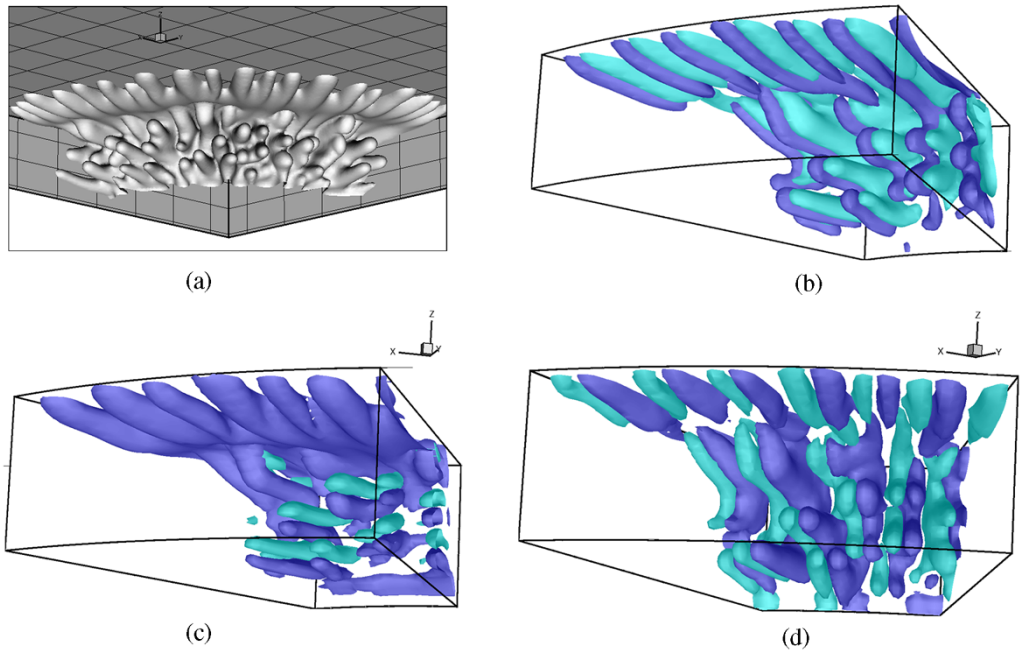


**Figure 3.** $G = 2$, $Pe = 800$, $R = 2.5$. Isosurfaces of (a) concentration, (b) horizontal viscous vorticity, (c) gravitational vorticity, (d) vertical viscous vorticity.



### 3.1. Gravity override

In the presence of density difference, the lower-density, injected fluid tends to rise above the heavier resident fluid, which leads to the formation of a gravity layer near the top boundary; figure 2(b). Increased flow rate in the gravity layer results in an effective local Peclet number higher than the average value and accelerates the growth of disturbances in this region. The interface tends to tilt forward in the displacement direction.

The formation of the gravity override region [8, 12], leads to less intense fingering in the lower layer, and bypass of resident fluid in the underride region. However, at a moderate $G = 0.5$ value, the underride fingers eventually develop and are subject to the buoyancy effect, which leads to their interaction with the gravity layer; figure 2(b). The type of this interaction can lie between two extremes:

(1) if the underride fingers pinch off the dominant fingers in the gravity layer, cutting their fluid supply, there can be a delay in the breakthrough time;

(2) if, on the other hand, the underride fingers merge with the gravity layer to increase its supply of less viscous fluid, the result can be a decrease in the breakthrough time.

The actual form that is realized depends upon the relative magnitude and spatial distribution of the viscous and gravitational vorticity.

A high value of $G = 2$ results in almost total elimination of underride fingers; figure 3(a). The gravity layer is dominant and interactions among fingers within the layer are more pronounced. The beneficial, type (1), interactions are absent; the interface is more tilted as compared to the previous case. Consequently the breakthrough time has reduced from 0.20 for $G = 0.5$ to 0.165 for $G = 2$.

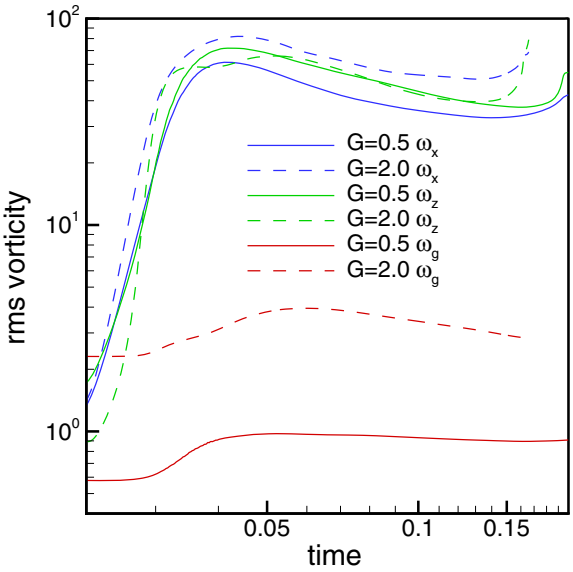


**Figure 4.** Vorticity rms values as a function of time for $G = 0.5$ and 2, $Pe = 800$, $R = 2.5$. The horizontal viscous component increases with $G$ but the vertical viscous component remains nearly independent of $G$ throughout the nonlinear phase.

In the 3D problem there are three spatial components of viscous vorticity and two spatial horizontal components of gravitational vorticity. The difference between horizontal and vertical components of viscous vorticity has important ramifications for the displacement process. Figure 3(b) shows the vertical viscous components for the case shown in figure 3(a), where the fingers are driven, primarily in the horizontal direction, by a structure of vorticity dipole pairs. The horizontal viscous component is shown in figure 3(c). Counterrotating vortex pairs are located next to each other, in horizontal planes for the vertical viscous component, shown in figure 3(b), and in the vertical planes for the horizontal viscous component, shown in figure 3(c). The gravitational vorticity dipole pairs, shown in figure 3(d), follow the orientation of the viscous vertical vorticity. The gravitational vorticity, although much smaller in magnitude than the viscous components, figure 4, makes an important contribution by changing the local concentration gradients, which strongly affects both the horizontal and vertical viscous components.

The evolution of vorticity is tracked by measuring the rms value as a function of time, as shown in figure 4 for two values of $G$. The effect of the increase in $G$ on the vertical and horizontal viscous components is worth noting. As $G$ is increased from 0.5 to 2, the vertical component remains unchanged and the horizontal component increases. This points to the positive (negative) correlation of horizontal (vertical) viscous vorticity with the gravity parameter. It follows, then, that the horizontal (vertical) viscous component reflects the influence of gravitational (viscous) effects.

### 3.2. Critical vorticity interaction

The efficiency of the displacement process can be defined as the volume of the displaced fluid produced at the production well up to breakthrough, as a fraction of the total domain volume. The type of coupling between the viscous and gravitational effects that can improve the efficiency by checking the growth of the gravity layer occurs at the right combination of parameters.

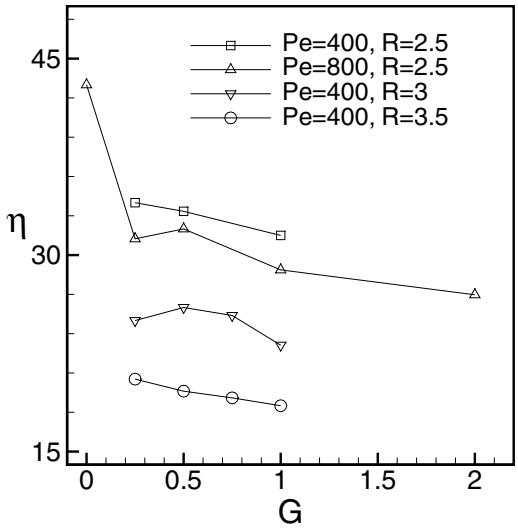


**Figure 5.** Efficiency curves for various regimes. A maximum for some parameter combinations indicates the favourable interaction between viscous and gravitational effects.

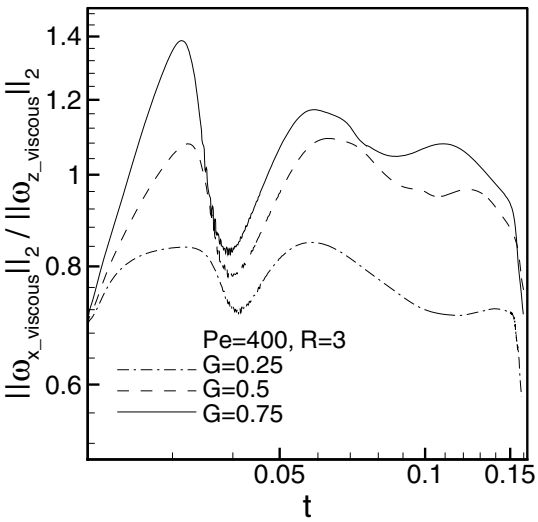


**Figure 6.** The rms value ratio of the horizontal to the vertical viscous vorticity. From figure 5, a maximum in efficiency occurs for $G = 0.5$ represented by successive dominance of each vorticity component.

Figure 5 plots the efficiency curves for various regimes. A maximum in the efficiency curve is observed for $Pe = 400, R = 3$ as $G$ goes from 0.25 to 0.75, while the efficiency decreases monotonically for the same combination as $R$ goes from 2.5 to 3.5. At $Pe = 800, R = 2.5$ there is a slight improvement in efficiency as $G$ goes from 0.25 to 0.5.

To get a better understanding of the gravity- and viscosity-related effects in the case where the efficiency is maximum, we plot in figure 6 the ratio of horizontal to vertical viscous vorticity for the case of $Pe = 400, R = 3, G = 0.25$–$0.75$.

For $G = 0.25$, the vertical viscous vorticity is dominant and the ratio is less than one. When $G = 0.5$, the horizontal component becomes larger than the vertical component for a brief period during the nonlinear phase but later the ratio drops below 1 again. As $G$ is increased to 0.75, the horizontal component is dominant for a longer period of time during the nonlinear phase. We conclude that the reason for the highest efficiency being at $G = 0.5$ is the fact that the initial dominance of vertical viscous vorticity develops the underride fingers and then later the dominance of buoyancy effects leads to their pinching off of the gravity layer. This does not happen at low $G$ when the gravity effect is not strong enough to lead to pinch-off and at high $G$ when the continued dominance of horizontal vorticity does not let the underride fingers develop to a point where any meaningful interaction with the gravity layer can be sustained.

## 4. Conclusions

From the above, we see that the interaction between spatial components of viscous and gravitational vorticity can have a substantial influence on the process efficiency. Although the magnitude of the gravity-related vorticity component is smaller than that of the viscosity-related component, it can combine with the horizontal viscous component to influence the displacement process. Therefore, we see that an increase in the gravity parameter is strongly correlated with the horizontal viscous component of the vorticity. For a favourable interaction, a delicate balance exists between the viscous and buoyancy effects where the viscous vorticity has to develop the underride fingers to sufficiently large amplitudes before buoyancy effects can lead to their interaction with the gravity layer. On the other hand, higher gravity values lead to an increased flow into the gravity layer right from the start, stabilizing the underride region, so the fingers in this region cannot have an appreciable effect on the gravity layer.

## References


[1] Homsy G M 1987 Viscous fingering in porous media *Annu. Rev. Fluid Mech.* **19** 271
[2] Hill S 1952 Channeling in packed columns *Chem. Eng. Sci.* **1** 247
[3] Saffman P G and Taylor G I 1958 The penetration of a fluid into a porous medium or Hele–Shaw cell containing a more viscous liquid *Proc. R. Soc.* A **245** 312
[4] Chouke R L, Meurs P V and Poel C V D 1952 The instability of slow, immiscible, viscous liquid–liquid displacements in permeable media *Trans. AIME* **216** 188
[5] Tan C T and Homsy G M 1988 Simulation of nonlinear viscous fingering in miscible displacement *Phys. Fluids* **31** 1330
[6] Chen C-Y and Meiburg E 1998 Miscible porous media displacements in the quarter five-spot configuration: part 1. The homogeneous case *J. Fluid Mech.* **371** 233
[7] Chen C-Y and Meiburg E 1998 Miscible porous media displacements in the quarter five-spot configuration: part 2. Effect of heterogeneities *J. Fluid Mech.* **371** 269
[8] Ruith M and Meiburg E 2000 Miscible rectilinear displacements with gravity override: part 1. Homogeneous porous medium *J. Fluid Mech.* **420** 225
[9] Manickam O and Homsy G M 1995 Fingering instability in vertical miscible displacement flows in porous media *J. Fluid Mech.* **288** 75
[10] Lele S K 1992 Compact finite differences with spectral-like resolution *J. Comput. Phys.* **103** 16
[11] Tan C T and Homsy G M 1986 Stability of miscible displacements in porous media: rectilinear flows *Phys. Fluids* **29** 3549
[12] Tchelepi H A and Orr F M J 1994 Interaction of viscous fingering, permeability inhomogeneity and gravity segregation in three dimensions *SPE Res. Eng.* **9** 266